PHYSICAL REVIEW B VOLUME 22, NUMBER 2 15 JULY 1980

Atomic structure of an impurity-stabilized Si{111} surface: Refinement using a combined-layer method

D. W. Jepsen
IBM T. J. Watson Research Center, Yorktown Heights, New York 10598

H. D. Shih and F. Jona
Department of Materials Science and Engineering, State University of New York, Stony Brook, New York 11794

P. M. Marcus
IBM T. J. Watson Research Center, Yorktown Heights, New York 10598

(Received 16 November 1979)

A low-energy electron diffraction (LEED) structure analysis of a Te-stabilized unreconstructed Si{111}1 × 1 surface is described. The intensity calculations were carried out with a computer program that treats multiple scattering in a unit made up of closely spaced surface or bulk layers in a spherical-wave expansion mode and then combines these units using a beam basis. Some details of an improved method of structure-constant evaluation employed in this program are described. The observed LEED intensities were compared with intensities calculated for several values of both the interlayer spacing and the inner potential. Quantitative comparison was made by the systematic use of the reliability factor of Zanazzi and Jona to yield both expectation values and confidence intervals. We find the separation of the first and second atomic layers to be $d_{12} = 0.62 \pm 0.03$ Å (bulk value 0.78 Å) and the inner potential, assumed to be energy independent, to be $V_0 = 11.7 \pm 0.9$ eV. The separation of the second and third layers is unchanged from the bulk value within about 1.5%.

I. INTRODUCTION

In a previous publication[1] we reported the preliminary results of a LEED (low-energy electron diffraction) structure analysis of an impurity-stabilized unreconstructed Si {111} surface. The stabilizing impurity was tellurium, and the resulting structure was believed to be similar to both the chlorine-stabilized 1 × 1 structure and the high-temperature 1 × 1 phase of the clean Si {111} surface reported earlier by Florio and Robertson.[2] An accurate solution of this structural problem is interesting on two accounts. Firstly, it provides direct information about the relaxation of a silicon surface, and thus makes reliable calculation of surface states possible,[3] while perhaps providing some guidance to the solution of the more complicated problem of surface reconstruction. Secondly, it increases confidence in the reliability of the layer-KKR (Korringa-Kohn-Rostoker) procedure and in the validity of the use of a muffin-tin potential model for the description of the scattering of an electron by covalent diamond lattice in LEED.

The preliminary results referred to above indicated that the unreconstructed Si {111} has a bulk-like structure, but some relaxation occurs. The first interlayer spacing (0.66 Å) was found to be about 15% contracted with respect to the interlayer spacing between equivalent {111} planes in the bulk (0.78 Å). Those results were obtained with a LEED intensity analysis employing a computer program, named HEX, which treats a Bravais surface layer in registry with, but at a variable distance from, the substrate, while the substrate is built up of double layers using beam methods. The comparison between calculated and observed intensities and the selection of the best fit were made visually, the usual procedure in LEED crystallography, and no systematic evaluation of the confidence limits was carried out.

The purpose of the present paper is to report the final results of a refinement of the same structure and to describe how such refinement was carried out. The LEED intensity calculations used a new computer program, named CHANGE, which is discussed in Sec. II. A brief description of the experimental procedures is given in Sec. III. The analysis of the data makes use of the reliability factor (the r factor) proposed by Zanazzi and Jona[4] for this purpose, and carries out a statistical evaluation of the confidence intervals for the final parameter values obtained. This analysis is described in Sec. IV. A brief discussion of the results is presented in Sec. V.

II. DISCUSSION OF THE COMPUTER PROGRAM

A. General procedures for combining layers

Most existing methods for calculating LEED intensities from multiple-scattering (or dynamical) diffraction theory make use of an expansion of the electron wave function between layers in terms of plane waves and exponentially increasing and decreasing waves at the given energy (usually called beams, in analogy with x-ray diffraction theory). These form a complete set of wave functions on any plane between the layers of the crystal parallel to the surface.[5-8] Some older work described the multiple scattering in terms of spherical waves which move from each of the atoms to each of the other atoms of the sample as well as to the detector.[9-13] More recently, a variation of this procedure using spherical waves has been developed by Zimmer and Holland[14] in which the scatters are separated into layers and the multiple scattering between layers is summed by an iterative procedure. The beam methods must also use spherical waves in a similar way to treat the multiple scattering inside each plane of atoms. In an obvious combination of these ideas one can treat a more complicated unit consisting of two or more closely spaced planes of atoms as a generalized layer and then combine these layer units using beam methods. This procedure was first suggested by Kambe,[15] who considered transfer-matrix methods for treating the beams between layers, and has been considered more recently by Tong and Van Hove[16] under the name of combined-space method using the matrix-doubling or renormalized-forward-scattering methods for performing the interlayer multiple scattering in the beam representation. We have obtained some previously published results using a procedure of this type,[17] which calculates the multiple scattering of a multilayer surface using spherical waves and then combines the scattering of this slab with the scattering of the bulk underneath by a transfer-matrix method in the beam representation. As has been explained by Kambe[15] and by Tong and Van Hove,[16] such a procedure combines the advantages of the spherical-wave representation and of the beam representation, while at the same time reducing some of the disadvantages of each of these procedures. The advantages of the spherical-wave basis are that it may be used when atoms lie in planes parallel to the surface which are very close together without affecting the convergence of the method. The disadvantage is that the calculation of structure factors and the inversion of the matrices, necessary to obtain the multiple scattering between layers, are both slow processes compared to the corresponding processes in beam methods. Using any of the beam methods one may calculate the dynamical theory for a slab crystal of 8 to 16 layers, or even for a semi-infinite crystal, in a much shorter time than one can do even a 5- to 7-layer crystal by the spherical-wave treatment. From five to eight phase shifts must be retained in describing the scattering of an atom in the LEED energy range. This leads to matrices of order 25 to 64 per layer which must be inverted in a spherical-wave method. The corresponding matrices in beam methods are usually somewhat smaller than this, but very large matrices must be employed when neighboring layers are close in comparison with the dimensions of the mesh in a layer.[18] At the higher energies of reflection-high-energy-electron diffraction (RHEED), where even more phase shifts are necessary to describe the scattering of an atom, the chain method of Pendry and Gard[19] for solving the multiple scattering between atoms in a layer is more efficient than the straightforward spherical-wave procedure. At present this procedure offers no advantage over other methods in the LEED range. (But see second paper of Ref. 19—note added in proof.)

In this work and in some other recent calculations, we have modified our previous program HEX so that it is also possible to treat closely spaced bulk layers in a spherical basis and then combine them using a beam basis. This new program CHANGE, is obviously useful for a structure such as that of the {111} face of silicon where the bulk planes are arranged as closely spaced pairs separated by a much larger distance. The program CHANGE treats up to six atoms in the surface mesh, arranged in one or more layers, in terms of spherical waves, and performs a similar calculation for the bulk with up to four atoms in each bulk unit cell. The program is restricted to bulk crystals which can be built up from groups of closely spaced adjacent layers where there is enough space between groups for the usual beam methods to be used. The scattering matrix of the bulk is obtained by performing the multiple scattering between groups of bulk layers by a transfer-matrix method. This scattering matrix of the bulk is then combined with that of the surface by the usual equations of the matrix-doubling method. The advantages of this program are its ability to handle closely spaced layers and its versatility, because in a single run many different surface structures can be tested, with different arrangements of atoms in planes and different orderings of planes in different structures. Its disadvantages is its low speed when complex layers are handled using spherical waves.

In general the ideas used in CHANGE, except for certain improvements in the use of the transfer matrix, have already been published by Kambe and by Tong and Van Hove.[9,10,12,16] However, in combining nearby layers using spherical waves, we use a new Ewald method for obtaining the structure factors for the scattering between layers which is a simplification of Kambe's treatment. This procedure will be described below. The improved method in using the transfer matrix used here will be presented in a future publication by one of the authors (DWJ).

B. Ewald method for scattering between layers

Kambe, in a series of three papers,[9,10,12] has given a treatment of the multiple scattering in a two-dimensional lattice of atoms, which adapts the KKR method for performing band-structure calculations[20] to the two-dimensional case. For evaluating the structure factors required in the KKR method, he developed an Ewald procedure which has quite different formulas from the usual three-dimensional Ewald procedure because of the intrinsic differences between two and three dimensions. The method is particularly valuable, since Shen and Krieger[21] have shown that Kambe's equations can be obtained from a variational procedure, so that the transmission and reflection coefficients obtained for a layer in this way are accurate to second order in the calculated coefficients of the wave function. The work of Kambe and of Shen and Krieger described above was carried through assuming that both the potential inside the atoms and the constant potential between the atoms are real, but the equations developed by Kambe are trivially generalizable to the situation in LEED where both of these potentials may have a negative imaginary part describing the incoherent scattering of electrons from the diffraction beams of the experiment. Kambe[12] has extended his treatment to handle a generalized layer of atoms in which a unit mesh of the layer may contain more than one atom, including the case in which different atoms in the unit mesh lie in different planes parallel to the surface. He also developed a generalized Ewald procedure for the structure factors required. A different, simpler, non-Ewald method was also proposed by Kambe for finding structure factors when the atoms are not in the same plane. This second method is actually a variation of the usual calculation of multiple scattering between layers by means of beams, which becomes inefficient and ultimately fails as the layers come close to each other. In most LEED calculations using a spherical basis the structure factors have been obtained by a direct summation in configuration space using the exponential decrease of the waves due to inelastic scattering to assure convergence, a procedure pioneered by Duke and Tucker.[13] However, in our tests the Ewald method was faster, particularly when a precision of more than two or three figures is desired or the amount of inelastic scattering is small. Pendry has reached a similar conclusion, although pointing out the greater programming effort required.[22]

Because of the greater speed of the Ewald method in the plane, we have improved the Ewald method given by Kambe for the structure factors for scattering between planes to give a similar fast procedure. We have used this new procedure for many-layer units both in the surface and the bulk of the crystal. The modification of Kambe's work necessary to achieve our improvement is small, but is not obvious from the previous work. We believe that it is a useful addition to the techniques of multiple-scattering theory in surfaces, particularly since Ewald techniques must be used when the amount of absorption is not large.

The calculation of the structure constants given by Kambe proceeds by a modification of the method of Ham and Segall[23] for the two-dimensional case. The structure constants $D_L^{(ij)}$ are given by the relation[24]

$$D_L^{(ij)} = -ip\sum_\alpha e^{i\vec{k}_0\cdot\vec{R}_\alpha} Y_L^*(\hat{W}_\alpha) h_l(p|\vec{W}_\alpha|)$$

or

$$D_L^{(ij)} = \lim_{|r|\to 0} \frac{1}{j_l(p|r|)} \int d\Omega_r Y_L^*(\hat{r}) G^{(ij)}(\vec{r}) , \qquad (1)$$

$$G^{(ij)}(\vec{r}) = -\sum_\alpha \frac{e^{i\vec{k}_0\cdot\vec{R}_\alpha} e^{ip|\vec{r}-\vec{W}_\alpha|}}{4\pi|\vec{r}-\vec{W}_\alpha|} , \quad i \neq j$$

with

$$\vec{W}_\alpha = \vec{R}_j - \vec{R}_i + \vec{R}_\alpha , \quad p = \sqrt{E} .$$

Here $L=(l,m)$ is an index labeling the allowed combinations of the indices l and m of the usual spherical harmonic Y_L as defined by Condon and Shortly,[25] R_i and R_j are vectors giving the positions of the ith and jth atoms of the basis in the unit mesh (two-dimensional cell), and $\{R_\alpha\}$ is the set of lattice vectors of the surface mesh (two-dimensional lattice). The quantity k_0 is the reduced wave vector of the electronic wave function in the plane of the surface. It is determined by the parallel component of $\vec{k}$ for the incoming wave, which in turn is fixed by the energy and direction of motion of the incident electron. The kinetic energy E in this formula is measured from the constant level of potential between the atoms, the so-called muffin-tin zero of potential, and includes a positive imaginary part arising from the negative imaginary term in the potential which describes the inelastic scattering of the electron in the crystal. In taking square roots in this paper we assume that the cut in the complex plane for the square-root function lies along the negative real axis, so that quantities like p that are square roots of complex numbers have positive real parts.

We shall evaluate Eq. (1) following the original method of Kambe quite closely. Using the procedure of Ham and Segall, Kambe writes the function G as an integral using the relation

$$\frac{e^{ipr}}{r}=\frac{1}{(2\pi)^{1/2}}\int_{0(C)}^{\infty}\zeta^{-1/2}\exp\left(-\tfrac{1}{2}r^2\zeta+\frac{p^2}{2\zeta}\right)d\zeta\,, \tag{2}$$

where (C) is a suitable contour.[23] Splitting the range of integration into the range from 0 to the Ewald parameter $2\mu^2$, and the range from $2\mu^2$ to ∞, one may divide the expression for the structure constants into two ζ integrals:

$$D_L^{(ij)}=\lim_{|r|\to 0}-\frac{1}{4\pi(2\pi)^{1/2}j_l(p|r|)}\int d\Omega_r Y_L^*(\hat{r})\left(\int_{0(C)}^{2\mu^2}d\zeta+\int_{2\mu^2}^{\infty}d\zeta\right)\zeta^{-1/2}\sum_{\alpha}e^{i\vec{k}_0\cdot\vec{R}_\alpha}\exp\left(-\tfrac{1}{2}(\vec{r}-\vec{W}_\alpha)^2\zeta+\frac{p^2}{2\zeta}\right). \tag{3}$$

The Ewald parameter is chosen in this form to simplify later equations.

The sum over α in the second integral over ζ converges rapidly because ζ is greater than $2\mu^2$. Hence this term can be used for the configuration-space part of an Ewald procedure. To obtain the $\vec{K}$-space part, the sum over α in the first integral, which represents a Bloch periodic function of r, is transformed by the Poisson summation formula (i.e., expressed as the sum of its Fourier series). This contribution then becomes a sum over all reciprocal lattice vectors $\vec{K}$ in the plane. After further manipulations one obtains for the first of these two integrals

$$\begin{aligned}D_L^{(ij)(1)}=&-\frac{i^m}{Ap^l}[2l+1)(l-m)!\,(l+m)!\,]^{1/2}\\&\times\sum_K e^{-i(\vec{K}+\vec{k}_0)\cdot(\vec{R}_j-\vec{R}_i)}e^{-im\phi(k_0+K)}\sum_{h=0}^{\frac{l-|m|}{2}}\left(\frac{|\vec{k}_0+\vec{K}|}{2}\right)^{|m|+2h}\frac{1}{h!\,(|m|+h)!}I_{l-|m|-2h}(K)\end{aligned} \tag{4}$$

with

$$I_n(\vec{K})=\frac{1}{n!}\int_{0(C')}^{\mu}\xi^{n-2}\exp(-Q\xi^{-2}-r_z^2\xi^2)H_n(\xi r_z)d\xi\,,$$

where $\phi(k_0+K)$ is the angle of $\vec{k}_0+\vec{K}$ from the x axis in the plane parallel to the surface, the quantity Q is given by

$$Q=[(\vec{k}_0+\vec{K})^2-E]/4\,,$$

r_z is the z component of the vector $\vec{R}_j-\vec{R}_i$ and is equal in magnitude to the distance between planes, A is the area of the unit mesh of atoms, and $H_n(x)$ is the usual Hermite polynomial.[26] The reduction to obtain Eq. (4) can be achieved by Kambe's procedures for obtaining the structure factors used in the scattering in a single plane,[27] and the use of the generating function of Hermite polynomials. The $I_n(K)$ defined here satisfies the recursion relation

$$\begin{aligned}I_{n+2}(K)&=\frac{1}{(n+1)(n+2)}[4QI_n(K)+\mathcal{K}_n(K)]\,,\\\mathcal{K}_n(K)&=-\frac{2}{n!}\mu^{n+1}H_n(\mu r_z)\exp(-Q\mu^{-2}-r_z^2\mu^2)\,.\end{aligned} \tag{5}$$

Initial values I_0 and I_1 for the recursion can be obtained from Eq. (4) in terms of error functions

$$\begin{aligned}I_0(K)=&\frac{e^{-2qr_z}}{2q}\operatorname{erfc}\left(\frac{q}{\mu}-r_z\mu\right)\\&+\frac{e^{2qr_z}}{2q}\operatorname{erfc}\left(\frac{q}{\mu}+r_z\mu\right),\\I_1(K)=&\,e^{-2qr_z}\operatorname{erfc}\left(\frac{q}{\mu}-r_z\mu\right)\\&-e^{2qr_z}\operatorname{erfc}\left(\frac{q}{\mu}+r_z\mu\right),\end{aligned} \tag{6}$$

with

$$q=\sqrt{Q}\,,\quad \operatorname{erfc}(z)=\int_z^{\infty}e^{-t^2}dt\,.$$

These last formulas can be verified by suitable variable substitutions in the error function integrals on the right-hand side.

In the second integral of Eq. (3), it is useful to split the sum over lattice vectors $\{R_\alpha\}$ into subsums over the groups of interatom vectors of equal length $S_A=|W_\alpha|$ called shells, followed by a sum over shells A. Thus the second integral is given by

$$\begin{aligned}D_L^{(ij)(2)}&=\sum_A Z_l(S_A)\Xi_L(S_A)\,,\\Z_l(S_A)&=\frac{1}{\pi(pS_A)^l S_A}\\&\quad\times\int_0^b\xi^{-2l-2}\exp(-\xi^{-2}+a^2\xi^2)d\xi\,,\end{aligned} \tag{7}$$

$$b=1/\mu S_A\,,\quad a=pS_A/2\,.$$

$$\Xi_L(S_A)=-\pi^{1/2}2^{l+1}\sum_{|R_\alpha|=S_A}\exp(i\vec{k}_0\cdot\vec{R}_\alpha)Y_L^*(\hat{W}_\alpha)\,,$$

where Ξ satisfies the recursion relations

$$\begin{aligned}\Xi_{lm}(S_A)=&\frac{-r_z}{S_\alpha}\left(\frac{(2l-1)(2l+1)}{l^2-m^2}\right)^{1/2}\Xi_{l-1m}(S_A)\\&-\left(\frac{(2l+1)[(l-1)^2-m^2]}{(2l-3)(l^2-m^2)}\right)^{1/2}\Xi_{l-2m}(S_A)\end{aligned} \tag{8}$$

starting with

$$\begin{aligned}\Xi_{mm}(S_A)&=\frac{(-1)^{m+1}[(2m+1)!]^{1/2}}{m!}[1-(r_z/S_A)^2]^{m/2}\\&\quad\times\sum_{|\vec{W}_\alpha|=S_A}e^{-im\phi(W_\alpha)}e^{i\vec{k}_0\cdot\vec{W}_\alpha},\\\Xi_{m-m}(S_A)&=-\frac{[(2m+1)!]^{1/2}}{m!}[1-(r_z/S_A)^2]^{m/2}\\&\quad\times\sum_{|\vec{W}_\alpha|=S_A}e^{im\phi(W_\alpha)}e^{i\vec{k}_0\cdot\vec{W}_\alpha},\end{aligned}\tag{9}$$

for $m \geq 0$. The quantity Z_l satisfies the recursion relation

$$\begin{aligned}Z_{l+1}(S_A)&=\frac{(l+\frac{1}{2})}{pS_A}Z_l(S_A)-\tfrac{1}{4}Z_{l-1}(S_A)\\&\quad+\frac{b^{-2l-1}}{2\pi(pS_A)^{l+1}S_A}\exp(-b^{-2}+a^2b^2)\end{aligned}\tag{10}$$

with Z_0 and Z_1 given by

$$\begin{aligned}Z_0(S_A)&=\frac{1}{\pi S_A}\int_0^b\xi^{-2}\exp(-\xi^{-2}+a^2\xi^2)d\xi\\&=\frac{1}{2\pi S_A}[e^{-2ia}\,\mathrm{erfc}(b^{-1}-iab)\\&\qquad+e^{2ia}\,\mathrm{erfc}(b^{-1}+iab)],\\Z_1(S_A)&=\frac{1}{\pi pS_A^2}\int_0^b\xi^{-4}\exp(-\xi^{-2}+a^2\xi^2)d\xi\\&=\frac{1}{2\pi pS_A^2}\Big((\tfrac{1}{2}+ia)e^{-2ia}\,\mathrm{erfc}(b^{-1}-iab)\\&\qquad+(\tfrac{1}{2}-ia)e^{2ia}\,\mathrm{erfc}(b^{-1}+iab)\\&\qquad+\frac{1}{b}\exp(-b^{-2}+a^2b^2)\Big).\end{aligned}\tag{11}$$

The integrals in the starting values for recursion can be obtained directly numerically or from standard procedures for obtaining the complex error function. For arguments away from the imaginary axis, the error function can be obtained from the continued fraction[28]

$$\begin{aligned}&u_m=z^2+2(m+1),\quad m\cong 20\\&u_{i-1}=z^2+2i-\tfrac{3}{2}-i(i-\tfrac{1}{2})/u_i,\\&\mathrm{erfc}(z)=\frac{ze^{-z^2}}{2u_0},\quad\mathrm{Re}(z)>0\\&\mathrm{erfc}(z)=\frac{ze^{-z^2}}{2u_0}+\sqrt{\pi},\quad\mathrm{Re}(z)<0.\end{aligned}\tag{12}$$

For arguments near the imaginary axis we have found the procedures given by Salzer[29] to be useful.

These results should be equivalent to those obtained by Kambe, although he did not give recursion relations in this form, and a detailed comparison has not been made. The principal new contribution made in this section is the recursion relation for $I_n(K)$ quoted above, which can be verified from the expression for $I_n(K)$ in Eq. (4). It can be combined with the recursion relation

$$\mathcal{H}_n(K)=(2\mu^2/n)[r_z\mathcal{H}_{n-1}(K)-\mathcal{H}_{n-2}(K)]\tag{13}$$

for the quantity $\mathcal{H}_n(K)$ to evaluate structure constants in a manner very similar to the procedure used to obtain the structure constants for scattering within a single layer. Procedures for calculating the structure factors for the scattering within a single layer by Kambe's methods are given by Pendry.[5] An alternate procedure for handling this case can be obtained by setting r_z equal to zero in the above formulas.

It might appear from these formulas that once the auxiliary quantities I, Z, and Ξ are obtained for the smaller angular momenta, structure factors for high l can be calculated by recursion with little extra effort. Unfortunately, we find that the lattice sums and reciprocal lattice sums converge more slowly for the higher l structure factors, so that the amount of work does increase substantially when the calculation is extended to obtain structure factors for large l. These procedures should be programmed with at least ten figures of precision because cancellation can occur between the configuration and $\vec{K}$-space parts of the Ewald procedure, particularly at the higher energies of LEED. Calculation for the bulk mesh and the surface mesh can be carried out together as suggested by Van Hove and Pendry.[30] In the $\vec{K}$-space part of the Ewald procedure, the surface mesh is built up from the bulk meshes.

III. EXPERIMENT

Since all of the important experimental details were given in the previous publication,[1] we only summarize here, for the convenience of the reader, the highlights of the experiment and add some clarifying remarks. The Si {111} substrate, from 20 Ω cm p-type material, was cleaned in the working chamber with a series of argon-ion bombardments and anneals until a well-developed LEED pattern of the 7×7 structure was obtained. In the final stage, the only impurity detectable on the surface by means of Auger-electron spectroscopy (AES) was carbon. In the customary doubly differentiated AES spectra the ratio between C line at 274 eV and the Si line at 92 eV was typically 2.5×10^{-3}.

The 7×7 structure was converted to 1×1 by the deposition of small amounts of tellurium and the subsequent resublimation of all but about 5% of one monolayer of the deposited amount. Three different procedures were eventually developed for the preparation of the impurity-stabilized 1×1 phase; they are described in the previous publication.[1] The final LEED pattern from which the intensity data were collected was of satisfactory visual quality with relatively low background and sharp spots on the fluorescent screen of a display-type equipment. The angular widths were estimated to vary between 1° and 1.5°. The intensity data (consisting of intensity *versus* energy of incident electrons) were collected sequentially by means of a brightness meter (spot photometer) aimed at the pertinent LEED spot on the fluorescent screen. Two sets of data were recorded: one at normal incidence, including the beams 10, $\bar{1}0$, 11, 20 and $\bar{2}0$, the other at $\theta = 8°$ and $\varphi = 0°$, including the beams 00, 10, $1\bar{1}$, $\bar{1}1$, $\bar{2}1$, and $\bar{2}0$, for a total of eleven spectra. For a precise definition of the diffraction angles θ and φ, and the consequent indexing of the LEED pattern, the reader is referred, e.g., to a recent review.[31] The unit mesh on the Si{111} surface was taken as having x and y axis along rows of atoms at 120° to one another. The experimental spectra were corrected for background and contact-potential difference between sample and electron-gun cathode and normalized to constant incident current of electrons.

The orientation of the second atomic layer with respect to the first was determined empirically, as described in Ref. 30, by comparing the experimental spectra with those calculated for a specific orientation of the second layer.

IV. STRUCTURE ANALYSIS

The intensity calculations were carried out with the CHANGE program described in Sec. II, using 8 phase shifts and 31 beams to describe the electron wave function. The surface layer and all bulk layers parallel to it were chosen to contain bases of two atoms (the two closely spaced atomic planes that are periodically encountered along a ⟨111⟩ direction of the diamond lattice). The real part of the Si potential was a muffin-tin potential produced from superposition of atomic charge densities in a fictitious Si crystal with fcc structure and muffin-tin radius 1.176 Å (i.e., one half the Si–Si distance in crystalline Si), because no program for carrying out the analogous procedure for the diamond lattice was available. The muffin-tin zero (the constant potential between spheres) or "inner potential" V_0 was varied in the course of the analysis in the process of matching theoretical to experimental curves. The imaginary part of the potential was assumed to be 3.0 eV, and the root-mean-square amplitude of the atomic vibrations $(\langle u^2 \rangle)^{1/2} = 0.10$ Å.

The parameters to be determined were the interplanar distance d_{12} between the first and second atomic planes in the surface layer (the corresponding distance in the interior of the crystal is 0.78 Å), and the inner potential V_0. At a later stage, some attention was also devoted to the sensitivity of the fit between theory and experiment to the interplanar distance d_{23} between second and third atomic planes (bulk value 3.14 Å). The refinement made use of the r factor proposed by Zanazzi and Jona.[4]

The analysis was carried out as follows. For each of the two angles of incidence at which data were collected ($\theta = 0°$ and $\theta = 8°$, $\varphi = 0°$) intensity calculations were carried out in which the value of d_{12} was varied around the value determined in the preliminary study[1] over a range of approximately 0.2 Å in steps of 0.05 Å, the inner potential V_0 being kept constant at 10.0 eV, expected to be near the correct value. Then, each theoretical spectrum was quantitatively compared to its experimental counterpart by calculating the value of the r factor for each curve. This was done for various displacements of the set of curves along the energy axis, corresponding to changes in V_0. For the nonnormal-incidence data the above procedure is, in a strict sense, incorrect because the refraction of the electron wave upon entering the solid requires a new intensity calculation for each different value of V_0, which is not equivalent to shifting the calculated spectrum along the energy axis. We performed several intensity calculations with different V_0 and d_{12} values, then determined the r factor for each of the calculated curves compared to the experimental ones.

For each spectrum i, either at normal incidence or off normal, we were therefore in a position to determine one value $d_{12}^{(i)}$ of the parameter d_{12} and one value $V_0^{(i)}$ of the inner potential V_0 for which the value $r_r^{(i)}$ of the reduced r factor was a minimum. For this determination we need not actually draw the r-factor contours in the (d_{12}, V_0) plane,[32] but simply locate the minimum as described elsewhere.[33] Thus, each experimental spectrum can be regarded as one measurement of the parameters to be determined (viz., d_{12} and V_0), and each set of spectra (one for $\theta = 0°$, the other for $\theta = 8°$, $\varphi = 0°$) can be regarded as a sample drawn from the universe whose mean is being sought.[34]

Table I lists, for each spectrum tested, the values of d_{12} and V_0 that minimize the corresponding r factor. Three spectra that were collected experimentally do not appear in the table ($\bar{1}0$ at $\theta = 0°$, 00 and $1\bar{1}$ at $\theta = 8°$, $\varphi = 0°$) because the calculated counterparts were found to be rather insensitive to variations of d_{12}, although the agreement with experiment was very good. The numbers in parentheses, in Table I, are the parameter values that minimize the r factor when we shift the curves calculated for fixed V_0 along the energy axis to

TABLE I. For each spectrum, the range ΔE over which experimental data are available, and the values of the inner potential V_0 and first interlayer spacing d_{12}, which minimize the corresponding r factor, are given. The numbers in parentheses are the values that minimize the r factor when the theoretical curves are shifted along the energy axis after calculation (see text).

Spectrum	ΔE (eV)	V_0 (eV)	d_{12} (Å)
		$\theta = 0°$	
10	123	12.6	0.59
11	88	10.8	0.63
20	69	10.1	0.66
$\bar{2}0$	71	10.4	0.63
	$\theta = 8°$	$\varphi = 0°$	
10	117	11.8 (11.8)	0.60 (0.60)
$\bar{1}1$	82	12.7 (12.8)	0.58 (0.59)
$\bar{2}1$	90	11.2 (11.1)	0.65 (0.65)
$\bar{2}0$	87	13.0 (13.3)	0.61 (0.56)

locate the minimum value of r. This procedure is not strictly correct (see above) but the numbers show that the results are very close to those obtained with the correct procedure followed above except for the case of the $\bar{2}0$ spectrum. With this exception, at least for $\theta = 8°$, it thus appears that the incorrect (but economical) procedure yields results similar to the correct (but expensive) procedure.

We can apply standard statistical formulas to the results listed in Table I to obtain mean values and standard deviations. We choose to weight the result provided by each spectrum according to the range ΔE_i of incident electron energy over which the spectrum was recorded. Thus,

$$\bar{Y} = \sum_{i=1}^{n} w_i Y_i \,, \qquad s_Y^2 = \left(\sum_{i=1}^{n} (Y_i - \bar{Y})^2 \right) \Big/ (n-1) \,, \tag{14}$$

where Y is either d_{12} or V_0,

$$w_i = \Delta E_i \Big/ \left(\sum_{i=1}^{n} \Delta E_i \right) ,$$

the sums extend over all n spectra in a given set, and s_Y is the estimated standard deviation of each Y_i.

The mean values obtained at 0° and 8° and their standard deviations s_s and s_v are

$$(\bar{d}_{12})_0 = 0.62\ \text{Å}, \quad (s_d)_0 = 0.03\ \text{Å},$$

$$(\bar{d}_{12})_8 = 0.61\ \text{Å}, \quad (s_d)_8 = 0.03\ \text{Å},$$

$$(\bar{V}_0)_0 = 11.2\ \text{eV}, \quad (s_V)_0 = 0.8\ \text{eV},$$

$$(\bar{V}_0)_8 = 12.1\ \text{eV}, \quad (s_V)_8 = 1.1\ \text{eV}.$$

A student's t test confirms that the two samples were indeed drawn from a single universe,[34] so that we can calculate the final mean value of each parameter Y and the related confidence interval with standard formulas[35]:

$$Y = \tfrac{1}{2}(\bar{Y}_0 + \bar{Y}_8) \pm t_{v,\alpha} \frac{s}{2} \left(\sum w_{0i}^2 + \sum w_{8\,i}^2 \right)^{1/2} , \tag{15}$$

where $\bar{Y}_0$ and $\bar{Y}_8$ are the mean values of Y found in the 0° and 8° sets, respectively, $w_{0\,i}$ and w_{8i} are the corresponding sets of weights, $t_{v,\alpha}$ is the t value for v degrees of freedom and α confidence level, n is the number of measurements in each set, and s^2 is the average of the two values of s_y^2 at 0° and 8°. We find at the 95% confidence level

$$d_{12} = 0.62 \pm 0.03\ \text{Å}, \quad V_0 = 11.7 \pm 0.9\ \text{eV}.$$

The spectra calculated with these parameters can be visually compared with their experimental counterparts in Figs. 1–3. The figures display the values of the individual r_r factors as well. The mean r factor $[\bar{r}_r = (\sum_i r_r^{(i)} \Delta E_i)/(\sum_i \Delta E_i)]$ for the whole structure is 0.25 for a total ΔE of 1099 eV. This value may be compared with the value 0.27

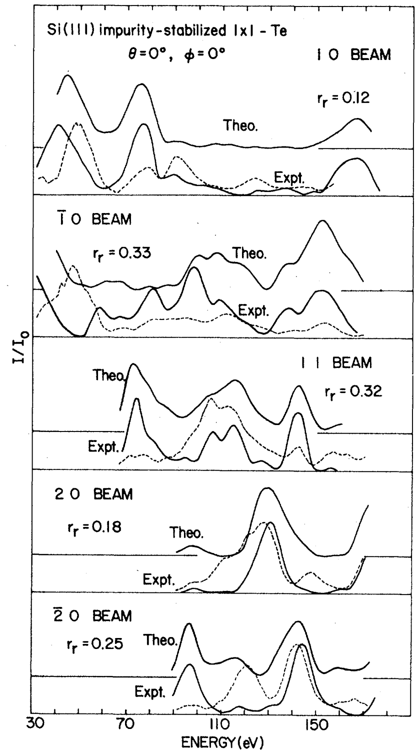

FIG. 1. Theoretical and experimental spectra (solid curves) for the impurity-stabilized Si {111} structure at normal incidence. The values of the r_r factor are listed in each panel. The dashed curves are the experimental spectra measured at normal incidence from an Si {111} 7×7 structure.

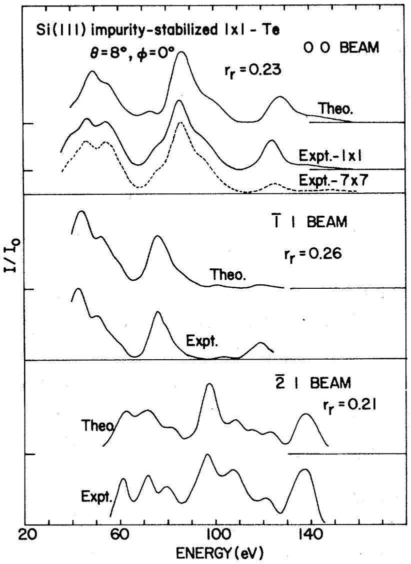

FIG. 2. Theoretical and experimental spectra (solid curves) for the impurity-stabilized Si{111} structure at $\theta = 8°$, $\varphi = 0°$. The values of the r_r factor are listed in each panel. The dashed curve in the upper panel is the 00 spectrum measured at the same incidence direction from an Si{111} 7× 7 structure.

for the structure of Ni{001}$c(2\times2)$–S, or the value 0.28 for the structure of Ag {001}$c(2\times2)$–Cl.[4] The structure R factor that takes into account the number of spectra used in the analysis[4] is 0.21.

In the later stages of refinement, we examined whether the theory-experiment correspondence and the $\bar{r}_r$ factor could be improved further by varying the second interplanar spacing d_{23}. We detected a tendency toward a slight expansion (by about 1.5%) of d_{23} with respect to its bulk value (3.14 Å), but the improvement was too small and not sufficiently uniform over all beams to warrant further analysis.

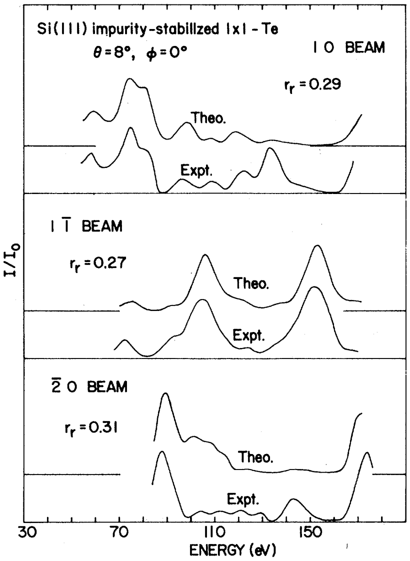

FIG. 3. Theoretical and experimental spectra for the impurity-stabilized Si{111} structure at $\theta = 8°$, $\varphi = 0°$. The values of the r_r factor are listed in each panel.

The quantitative analysis described above did not take into account the effect of errors (or changes) in the experimental scattering geometry, in particular, the diffraction angle θ. However, the effect was investigated semiquantitatively by visual comparison among pertinent LEED spectra as follows. First, it was established that corresponding spectra calculated for $\theta = 6°$, 7°, 8°, 9°, and 10° did not differ much from one another, i.e., small changes in the incidence angle did not substantially affect the curves. (This relative insensitivity of spectra to small changes in θ is more the rule than the exception, although of course it cannot be taken for granted in all cases.) Second, it was established visually that the set calculated for $\theta = 8°$ did in fact agree best with experiment, thus giving us confidence that the diffraction angle had been measured correctly.

The error bars given here are somewhat narrower than those quoted in typical LEED studies, and this may lead some readers to ask whether they are indeed a measure of the accuracy of the work, or, at best, a measure of the precision with which the measurements were carried out. The methodology of LEED is still too new and untested to be sure that these numbers indeed measure the error, but we believe that they have some significance in this regard for the following reason: In an earlier stage of this work, the data for $\theta = 0°$ gave slightly different results for V_0 and d_{12} than the $\theta = 8°$ data. In fact, the results were different enough to lie outside each other's error bars, indicating some type of systematic error. This discrepancy was later eliminated by increasing the number of phase shifts used in the calculation from five to eight, although, to the eye, this refinement produced only very small changes in the curves. Thus, to achieve the consistent error estimates given here, quite accurate calculations had to be compared with the experiment. We believe that a systematic error in the measurements would also have shown up in the statistics as a similar discrepancy.

V. DISCUSSION

Three comments seem appropriate after the conclusion of the structural refinement reported above. The first relates to the nature of an impurity stabilized Si $\{111\}$ 1×1 surface. One striking fact about this surface is that, although the LEED pattern exhibits a clear 1×1 character, the energy spectra for the integral order beams are similar to those from the Si 7×7 structure, as has been remarked before.[2] In this situation one may ask whether one is really seeing antiphase domains of the Si 7×7 structure which are sufficiently small that many domains lie within the area of coherence of the experiment. Each impurity atom might anchor a small region of 7×7 structure placed so that the impurity atom lies in a particular position in the structure, with the result that a random arrangement of impurities gives a random collection of incoherently placed domains. It is easy to see in kinematic theory that the Huygens' wavelets from different antiphase domains will add constructively to give the integral order beams, whereas they will add destructively for the fractional order beams and cancel exactly if all of the possible domains occur with equal area. A higher background would be expected from the domain effects in the fractional spots, i.e., very broadened fractional spots. The same results will be true in a dynamical theory which is simplified by requiring that multiple scattering only occur within the separate domains.

At present, there is no evidence that this phenomenon occurs in actual systems. It would be useful to perform experiments in which the coherence length is increased significantly above present sizes to see whether the fractional order spots can be broadened and reduced in intensity relative to the integral order beams in some system where experiments with shorter coherence length have shown typical bright fractional order spots.

We have concluded that small antiphase domains of Si 7×7 are not likely in the present system for the following reasons: (i) The effect is not so likely here because the 7×7 mesh is so large. There would have to be seven different displacements of the antiphase domains along both the x and y axis of the pattern in order to cancel the seventh-order spots which occur in the pattern in these directions. This is a large number of 7×7 domains to fit into the coherence area, and the deviations from the equal area of different domains would give fractional order spots. (ii) The background in the observed 1×1 LEED pattern is low, whereas the small domains and the distortions that undoubtedly would occur at the boundaries between antiphase domains would be expected to produce a noticeable background. (iii) There are significant, albeit sometimes small, differences between the integral-order LEED spectra measured on the 1×1 and the 7×7 structure. We have drawn the 7×7 spectra in Figs. 1 and 2 (dashed curves) so that they can be compared with the corresponding 1×1 spectra. It is striking that the 00 spectra (at $\theta = 8°$) are almost identical to one another, and it may be significant that the 00 spectrum of the cleaved 2×1 structure is also somewhat similar.[36] The nonspecular LEED spectra, however, are notably different. To avoid subjectivity, we have determined the r-factors for the comparison between corresponding 1×1 and 7×7 spectra. The results are, for the $\theta = 0°$ data, the following: 10 spectrum, $r_r = 0.63$; $\bar{1}0$ spectrum, $r_r = 0.64$; 11 spectrum, $r_r = 1.25$; 20 spectrum, $r_r = 0.42$; and $\bar{2}0$ spectrum, $r_r = 0.72$. For the $\theta = 8°$ data we have 00 spectrum, $r_r = 0.08$. Hence, we conclude that the structure investigated here is *not* a broken up 7×7 structure.

It has also been suggested[37] that the structure might be a random arrangement of subunits which normally fit together in a definite pattern to give the 7×7 structure. This is harder to exclude than domains of the full 7×7 structure since the integral beams would not be the same as those of the 7×7, there would be fewer fractional order spots to blur away, and smaller-sized elements to fit into the coherence area of the measurement. Furthermore, such a structure could well have lower energy than a true 1×1 structure because it could be put together with fewer dangling bonds. If this is assumed to be the structure, then we believe that this study has determined the correct interlayer spacings of that structure, with the random elements of the structure being displacements of atoms within these planes. The incident beam and the measured beams in this work were all at angles less than 30° from the normal and, therefore, the data are probably much more sensitive to displacements perpendicular to the surface than to parallel displacements.

The second comment relates to the methodology of LEED crystallography and the associated error analysis. The Si $\{111\}$ 1×1 structure discussed here is the first published surface structure for which the refinement was carried out exactly in the manner described above. The r-factor has been used for structural refinement by other workers[32,38,39] as well, but in a somewhat different way. We believe that the procedures outlined here are better suited for a statistical analysis of the confidence levels.

The third comment concerns the structure of the unreconstructed, impurity-stabilized Si $\{111\}$ 1×1 surface as determined in this work. This structure is essentially bulklike, but with a contraction of the first interplanar spacing d_{12} by about 21%. This contraction is much smaller than the 42% that was suggested earler on the basis of Pauling's bond-order versus bond-length formula.[3] It agrees well with the calculation of this spacing by Ihm and Cohen.[40] It is somewhat smaller than the 24% that was "ruled out" by Appelbaum and Hamann (AH) on the basis of comparison between theoretical predictions and experiment. The theoretical predictions concerned surface-state critical points and surface resonances on the 1×1 surface, while the experiments consisted of photoemission and energy-loss spectra from the Si $\{111\}$ 7×7 structure.[3] AH carried out self-consistent electronic structure calculations of a number of surface properties for two other geometries of the unreconstructed surface, viz., a contraction of d_{12} by about 44.5% and the same contraction of d_{12} added to a small contraction of d_{23} of about 4.5%. These drastic distortions were found to have little effect on either ionization potential or Fermi energy but large influences on surface state bands. It is not clear why such large distortions were required. Perhaps the goal was to match theoretical results for Si $\{111\}$ 1×1 with experimental results for Si $\{111\}$ 7×7. It is questionable, however, whether such a goal is justified, because the difference between the 1×1 and 7×7 structures is perhaps larger than heretofore believed (see Figs. 1–3 and above discussion). Unfortunately, Ihm and Cohen[40] did not discuss the surface states. One might assume that the impurity-stabilized 1×1 structure determined here is indeed the same as the clean 1×1 structure produced at high temperatures, but this assumption has never been tested. It would appear instructive to calculate surface states for a 1×1 structure with a 21% contraction as determined here and to compare the results with photoemission spectra measured on an impurity-stabilized unreconstructed surface.

ACKNOWLEDGMENTS

Two of the authors (H.D.S. and F.J.) acknowledge gratefully the partial sponsorship of this work by the National Science Foundation. Particular thanks are due to Stephen Finch, of the Department of Applied Mathematics and Statistics at Stony Brook, for his patient coaching and advice in matters of error analysis.

---

[1] H. D. Shih, F. Jona, D. W. Jepsen, and P. M. Marcus, Phys. Rev. Lett. 37, 1622 (1976).

[2] J. V. Florio and W. D. Robertson, Surf. Sci. 24, 173 (1971).

[3] J. A. Appelbaum and D. R. Hamann, Phys. Rev. Lett. 31, 106 (1973); 32, 225 (1974).

[4] E. Zanazzi and F. Jona, Surf. Sci. 62, 61 (1977).

[5] J. B. Pendry, *Low Energy Electron Diffraction* (Academic, New York, 1974).

[6] M. A. Van Hove and S. Y. Tong, *Surface Crystallography by LEED* (Springer, New York, 1979).

[7] E. G. McRae and P. J. Jennings, Surf. Sci. 15, 345 (1969).

[8] D. W. Jepsen and P. Marcus, in *Computational Methods in Band Theory*, edited by P. M. Marcus, J. F. Janak, and A. R. Williams (Plenum, New York, 1971); D. W. Jepsen, P. M. Marcus, and F. Jona, Phys. Rev. B 5, 3933 (1972).

[9] K. Kambe, Z. Naturforsch. 22a, 322 (1967).

[10] K. Kambe, Z. Naturforsch. 22a, 422 (1967).

[11] J. L. Beeby, J. Phys. C 1, 82 (1968).

[12] K. Kambe, Z. Naturforsch. 23a, 1280 (1968).

[13] C. B. Duke and C. W. Tucker, Phys. Rev. Lett. 23, 1163 (1969); Phys. Rev. B 3, 3561 (1971).

[14] R. S. Zimmer and B. W. Holland, J. Phys. C 8, 2395 (1975).

[15] Reference 12, Sec. 8.

[16] S. Y. Tong and M. A. Van Hove, Phys. Rev. 16, 1459 (1977).

[17] H. D. Shih, F. Jona, D. W. Jepsen, and P. M. Marcus, Commun. on Phys. 1, 25 (1976); F. Jona, A. Ignatiev, D. W. Jepsen, and P. M. Marcus, Bull. Am. Phys. Soc. II 1 20, 407 (1975); F. Jona, Surf. Sci. 68, 204 (1977).

[18] Reference 5, p. 141; Ref. 16, Sec. II.

[19] J. B. Pendry and P. Gard, J. Phys. C 8, 2048 (1975); N. Masud, C. G. Kinniburgh, and D. J. Titterington, J. Phys. C 12, 5263 (1979).

[20] B. Segall and F. S. Ham, in *Methods in Computational Physics*, Vol. 8, edited by B. Alder, S. Fernbach, and M. Rotenberg (Academic, New York, 1968), pp. 251–299.

[21] A. P. Shen and J. B. Krieger, Phys. Rev. B 3, 4189 (1971).

[22] Reference 1, p. 152.

[23] F. S. Ham and B. Segall, Phys. Rev. 124, 1786 (1961), Sec. VII.

[24] Reference 9, Eq. (3.10).

[25] E. U. Condon and G. H. Shortley, *The Theory of Atomic Spectra* (Cambridge Univ. Press, London, 1935).

[26] A. Erdelyi, W. Magnus, F. Oberhettinger, and F. G. Tricomi, *Higher Transcendental Functions* (McGraw-Hill, New York, 1953), p. 192.

[27] Reference 9, Appendix I; see also corrections in Ref. 12.

[28] B. D. Fried and S. D. Conte, *The Plasma Dispersion Function* (Academic, New York, 1961); H. S. Wall, *Continued Fractions* (Van Nostrand, New York, 1948), p. 357; M. Abramowitz and I. A. Stegun, *Handbook of Mathematical Functions* (National Bureau of Standards, Washington, 1964), p. 298.

[29] H. E. Salzer, Math. Tab. Aid. Comp. 35, 67 (1951).

[30] M. A. Van Hove and J. B. Pendry, J. Phys. C 8, 1362

(1975), Sec. 3.

[31] F. Jona, J. Phys. C 11, 4271 (1978).

[32] P. R. Watson, F. R. Shepherd, D. C. Frost, and K. A. R. Mitchell, Surf. Sci. 72, 562 (1978).

[33] F. Jona and H. D. Shih, J. Vac. Sci. Technol. 16, 1249 (1979).

[34] R. H. Bacon, in *The Lloyd William Taylor Manual of Advanced Undergraduate Experiments in Physics*, edited by T. B. Brown (Addison-Wesley, Reading, Mass., 1959), pp. 1–28.

[35] See, e.g., Murray R. Spiegel, *Statistics*, Schaum's Outline Series (McGraw-Hill, New York, 1961), p. 188 *et seq.*; Samuel S. Wilks, *Mathematical Statistics* (Wiley, New York, 1962), p. 83.

[36] W. Monch and P. P. Auer, J. Vac. Sci. Technol. 15, 1230 (1978).

[37] D. E. Eastman, J. Vac. Sci. Technol. (to be published).

[38] H. L. Davis, J. R. Noonan, and L. H. Jenkins, Surf. Sci. 83, 559 (1979).

[39] R. W. Streater, W. T. Moore, P. R. Watson, D. C. Frost, and K. A. R. Mitchell, Surf. Sci. 72, 744 (1978).

[40] J. Ihm and M. L. Cohen, Solid State Commun. 29, 711 (1979).